

# Partitioned Component Mode Synthesis via a Flexibility Approach

K. C. Park\*

University of Colorado, Boulder, Colorado 80309-0429

and

Yong Hwa Park†

Samsung Electronics Company, Ltd., Suwon City, Republic of Korea

Q1

A new flexibility-based component mode synthesis method is presented, which is derived by approximating the partitioned equations of motion that employ a localized method of Lagrange multipliers. The use of the localized Lagrange multipliers leads to, unlike the classical Lagrange multipliers, a linearly independent set of interface forces without any redundancies at multiply connected interface nodes. Hence, the resulting interface flexibility matrices are uniquely determined and well suited for the present method development. An attractive feature of the present method is its substructural mode selection criterion that is independent of loading conditions. Numerical experiments show that the present modal selection criterion is reliable and that the proposed flexibility-based component mode synthesis method performs well relative to the classical Craig-Bampton method in terms of accuracy and of its ability to include dominant substructural modes for simple plates and a relatively complex solid ring.

Q2

## Nomenclature

$B$  = interface constraint compatibility Boolean matrix  
 $C$  = damping matrix,  $N (m/s)^{-1}$ , or  $N \cdot m (rad/s)^{-1}$   
 $d$  = deformation part of the displacement,  $m$  or  $rad$   
 $F$  = flexibility matrix,  $m/N$  or  $rad/N \cdot m$   
 $\mathcal{F}$  = composition of flexibility matrix, either inertia or stiffness attribute  
 $f$  = substructural applied force vector,  $N$  or  $N \cdot m$   
 $f_g^D$  = D'Alembert's force vector,  $N$  or  $N \cdot m$   
 $I$  = identity matrix  
 $K$  = stiffness matrix,  $N/m$  or  $N \cdot m$   
 $L$  = assembly Boolean matrix  
 $M$  = mass matrix,  $kg$   
 $q$  = generalized coordinates of the deformation vector,  $m$  or  $rad$   
 $R$  = rigid-body mode shape matrix  
 $r$  = rigid-body part of the displacement,  $m$  or  $rad$   
 $u$  = substructural displacement vector,  $m$  or  $rad$   
 $u_g$  = global displacement vector,  $m$  or  $rad$   
 $\alpha$  = generalized coordinates of the rigid-body motion vector,  $m$  or  $rad$   
 $\Lambda$  =  $\text{diag}\{\omega_{n1}^2, \omega_{n2}^2, \dots, \omega_{nm}^2\}$ ,  $(rad/s)^2$   
 $\lambda_\ell$  = localized interface Lagrange multipliers,  $N$  or  $N \cdot m$   
 $\Phi$  = deformation mode shape matrix  
 $\omega$  = natural or forcing frequency,  $rad/s$

$m$  = mass or inertial attribute  
 $r$  = residual mode degrees of freedom  
 $s$  = stiffness attribute  
 $\alpha$  = rigid-body degrees of freedom

## Superscripts

$D$  = D'Alembert or dynamic attribute  
 $S$  = Schur complement of a matrix  
 $T$  = transposition of a matrix

## Subscripts

$b$  = interface boundary degrees of freedom  
 $d$  = deformation mode degrees of freedom  
 $g$  = assembled global degrees of freedom or global attribute  
 $\ell$  = localized (or substructural) variable

## Introduction

SIMPLIFIED structural models are essential for a variety of reasons: shock isolation systems design, active vibration controller design, system identification and experimentally verified model development, and health monitoring of transportation infrastructures. Most existing methods work well for their intended applications, and the choice of a particular method depends largely on the experience and preference of the dynamics specialists. There exists one consensus among the dynamics specialists: The model reduction of each substructure still relies on a rule of thumb or paradigm, that is, retain the substructural modes about twice the global modes that need to be modeled in the overall system.

In recent years several new developments have been emerging wherein this rule of thumb is not only inadequate but also can lead to grave consequences. Examples include distributed and/or localized active control of structural systems, structure-medium interaction systems, model-based structural health monitoring, and structures that consist of substructures whose response timescales are widely varying. First, at present there is a general agreement among the researchers in structural dynamics that the relative strength, shortcomings, similarities, and implementation aspects of existing component mode synthesis methods<sup>1-10</sup> are well understood. What is not well understood or developed is a rational selection of modes in each substructure for each specific model construction. This is especially relevant when the eigenvalue analysis of substructures can be carried out in individual processors of a parallel computer, yet substantially reduced-order models are desired. Second, although a variety of parallel computational algorithms have been developed for quasi-static and transient response structural analysis,<sup>11-15</sup> it is generally agreed that the state of parallel structural eigenvalue analysis in terms of parallel scalability is in an evolving stage.

Received 2 November 2002; revision received 22 October 2003; accepted for publication 18 November 2003.

Copies of this paper may be made for personal or internal use, on condition that the copier pay the \$10.00 per-copy fee to the Copyright Clearance Center, Inc., 222 Rosewood Drive, Danvers, MA 01923; include the code 0001-1452/04 \$10.00 in correspondence with the CCC.

\*Professor, Center for Aerospace Structures and Department of Aerospace Engineering Sciences; kcpark@colorado.edu. Associate Fellow AIAA.

†Senior Engineer, Visual Display Division, Digital Multimedia Network, 416 Maechang-dong; yongh.park@samsung.com.

Q3

The preceding observations have motivated the present authors to derive a family of component mode synthesis methods with error assessment expressions so that the model reduction process can be automated in parallel computations. In doing so, the present paper is a theoretical attempt to substitute the word heuristic by rational in Meirovitch's statement<sup>8</sup> regarding the component mode synthesis: "The component-mode synthesis represents a sound heuristic, physically motivated approach to the dynamics of structures. . . unlike the assumed-modes method which could invoke the Rayleigh-Ritz theory to claim convergence, the component-mode synthesis cannot make such claims." Note that most of the existing component-mode synthesis methods have relied on a bottom-up approach: First approximate each substructure, then assemble the approximated substructural equations to form the reduced global equations of motion.

The present method adopts a top-down approach: First, begin with the full global equations of motion; second, partition them into substructures as if each of the partitioned substructures are completely free; third, select a reduced set of modes for each substructure according to the mode selection criterion proposed herein and approximate the residual modes that are not included in the reduces basis set; fourth, augment the total virtual work of completely free substructures with the partition interface conditions via a localized method of Lagrange multiplier; and fifth, carry out the reduced eigenvalue problem.

The vehicle for carrying out the five steps is a partitioned formulation that involve four independent variables: the rigid-body modes of each substructure, the substructural deformation modes, the Lagrange multipliers that represent the interface generalized force vector, and the interface nodal displacements. By the elimination of some of the four-field variables, several forms of the exact eigenvalue analysis equations are specialized. Because the exact eigenvalue analysis equations are computationally intractable, approximations are introduced, each with the corresponding error assessment expressions. Of several component-mode synthesis methods derived from the present formalisms, we focus on the flexibility-based synthesis method because it offers improved accuracy and potential applications to parallel computations. The performance of the present flexibility-based component mode synthesis method along with the substructural mode selection criterion is demonstrated via two simple problems and one moderately complex problem.

### Partitioning of Global Structural Dynamics Equation

The displacement-based discrete energy functional  $\Pi(\mathbf{u}_g)$  for a linear structure under dynamic loads can be expressed as

$$\Pi(\mathbf{u}_g) = \mathbf{u}_g^T \left( \frac{1}{2} \mathbf{K}_g \mathbf{u}_g - \mathbf{f}_g^D \right), \quad \mathbf{f}_g^D = \mathbf{f}_g - \mathbf{M}_g \ddot{\mathbf{u}}_g - \mathbf{C}_g \dot{\mathbf{u}}_g$$

$$\mathbf{K}_g = \mathbf{L}^T \mathbf{K} \mathbf{L}, \quad \mathbf{M}_g = \mathbf{L}^T \mathbf{M} \mathbf{L}, \quad \mathbf{C}_g = \mathbf{L}^T \mathbf{C} \mathbf{L} \quad (1)$$

Observe that, if no domain decomposition is contemplated, the preceding functional leads to the well-known global linear structural dynamics equation, namely,

$$\delta \Pi(\mathbf{u}_g) = 0 \Rightarrow \mathbf{M}_g \ddot{\mathbf{u}}_g + \mathbf{C}_g \dot{\mathbf{u}}_g + \mathbf{K}_g \mathbf{u}_g = \mathbf{f}_g \quad (2)$$

where it is understood that the d'Alembert variable  $\ddot{\mathbf{u}}_g$  does not participate in the variational process.

Now consider the example of an assembled continuum structure partitioned into individual elements as shown in Fig. 1. The individual nodal displacements  $\mathbf{u}$  are related to the assembled global displacements  $\mathbf{u}_g$  through the assembly matrix  $\mathbf{L}$  according to

$$\mathbf{u} - \mathbf{L} \mathbf{u}_g = 0, \quad \mathbf{u} = \begin{bmatrix} \mathbf{u}_I^A & \mathbf{u}_\Gamma^A & \mathbf{u}_I^B & \mathbf{u}_\Gamma^B \end{bmatrix}^T \quad (3)$$

where superscripts *A* and *B* indicate the substructures and subscripts *I* and  $\Gamma$  denote interior and interface degrees of freedom (DOF), respectively. Hence, the discrete energy functional can be expressed

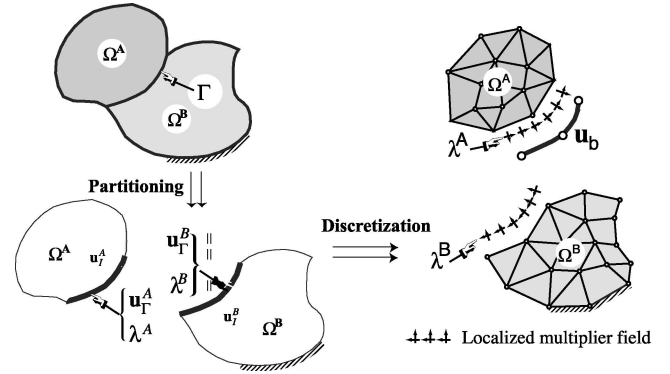


Fig. 1 Partitioning of a continuum into substructures.

in terms of the partitioned elemental displacements as

$$\Pi(\mathbf{u}_g, \lambda_\ell, \mathbf{u}) = \mathbf{u}_g^T \left( \frac{1}{2} \mathbf{L}^T \mathbf{K} \mathbf{L} \mathbf{u}_g - \mathbf{L}^T \mathbf{f}^D \right)$$

$$= \mathbf{u}^T \left( \frac{1}{2} \mathbf{K} \mathbf{u} - \mathbf{f}^D \right) + \lambda_\ell^T \mathbf{B}^T (\mathbf{u} - \mathbf{L} \mathbf{u}_g)$$

$$\mathbf{f}^D = \mathbf{f} - \mathbf{M} \ddot{\mathbf{u}} - \mathbf{C} \dot{\mathbf{u}} \quad (4)$$

where  $\mathbf{B}$  is a Boolean matrix that extracts the interface boundary DOF such that it enforces the interelement kinematical compatibility condition in Eq. (3).

Note that the present kinematical constraint condition equation (3) leads to a localized characterization of the Lagrange multipliers.<sup>16-18</sup> The difference between the classical and the present localized  $\lambda$  methods is illustrated in Fig. 2 for the case of four bodies (or nodes) partitioned. Note that the kinematic constraint condition by the classical  $\lambda$  method relates the partitioned nodes along one domain directly to its neighboring ones. On the other hand, the localized  $\lambda$  method relates every partitioned node to a reference node (or assembled node). In other words, the classical Lagrange multipliers interconnect the substructural boundary DOF directly, which leads to coupled interface residual flexibility in subsequent derivations. In contrast, the localized Lagrange multipliers do not directly connect the interface DOF. Hence, the resulting interface residual flexibility is completely uncoupled from substructure to substructure. This feature plays an important role in approximating the exact transcendental frequency equations.

### Four-Variable Partitioned Equations of Motion

The constrained energy functional derived in Eq. (4) can be further decomposed by expressing the substructural displacements  $\mathbf{u}$  in two parts:

$$\mathbf{u} = \mathbf{d} + \mathbf{r}, \quad \ddot{\mathbf{u}} = \ddot{\mathbf{d}} + \ddot{\mathbf{r}}$$

$$\mathbf{d} = \Phi \mathbf{q}, \quad \Phi^T \mathbf{M} \Phi = \mathbf{I}_\Phi, \quad \mathbf{R}^T \mathbf{M} \Phi = \mathbf{0}$$

$$\mathbf{r} = \mathbf{R} \alpha, \quad \mathbf{K} \mathbf{R} = \mathbf{0}, \quad \mathbf{R}^T \mathbf{M} \mathbf{R} = \mathbf{I}_\alpha \quad (5)$$

Substituting Eq. (5) into Eq. (4) leads to

$$\Pi(\lambda_\ell, \alpha, \mathbf{q}, \mathbf{u}_g) = \mathbf{q}^T \Phi^T \cdot \left[ \frac{1}{2} \mathbf{K} \Phi \mathbf{q} - \mathbf{f} + \mathbf{M} (\Phi \ddot{\mathbf{q}} + \mathbf{R} \ddot{\alpha}) \right.$$

$$\left. + \mathbf{C} (\Phi \dot{\mathbf{q}} + \mathbf{R} \dot{\alpha}) \right] + \lambda_\ell^T \mathbf{B}^T \cdot (\Phi \mathbf{q} - \mathbf{L} \mathbf{u}_g)$$

$$+ \alpha^T \mathbf{R}^T \cdot [-\mathbf{f} + \mathbf{M} (\Phi \ddot{\mathbf{q}} + \mathbf{R} \ddot{\alpha}) + \mathbf{C} (\Phi \dot{\mathbf{q}} + \mathbf{r} \dot{\alpha}) + \mathbf{B} \lambda_\ell] \quad (6)$$

Note that the four state variables,  $\mathbf{q}$ ,  $\lambda_\ell$ ,  $\alpha$ , and  $\mathbf{u}_g$ , in Eq. (6) are linearly independent provided that the constraint matrix  $\mathbf{B}$  has full column rank. In other words, it is variationally complete.

Noting that the virtual kinetic energy of the cross-coupling term between the deformation modes and the rigid-body modes would be zero, we have

$$\delta \mathbf{q}^T \Phi^T \mathbf{M} \mathbf{R} \ddot{\alpha} = \delta \mathbf{q}^T \Phi^T \mathbf{M} \mathbf{R} \ddot{\alpha} = \mathbf{0} \quad (7)$$

Q4

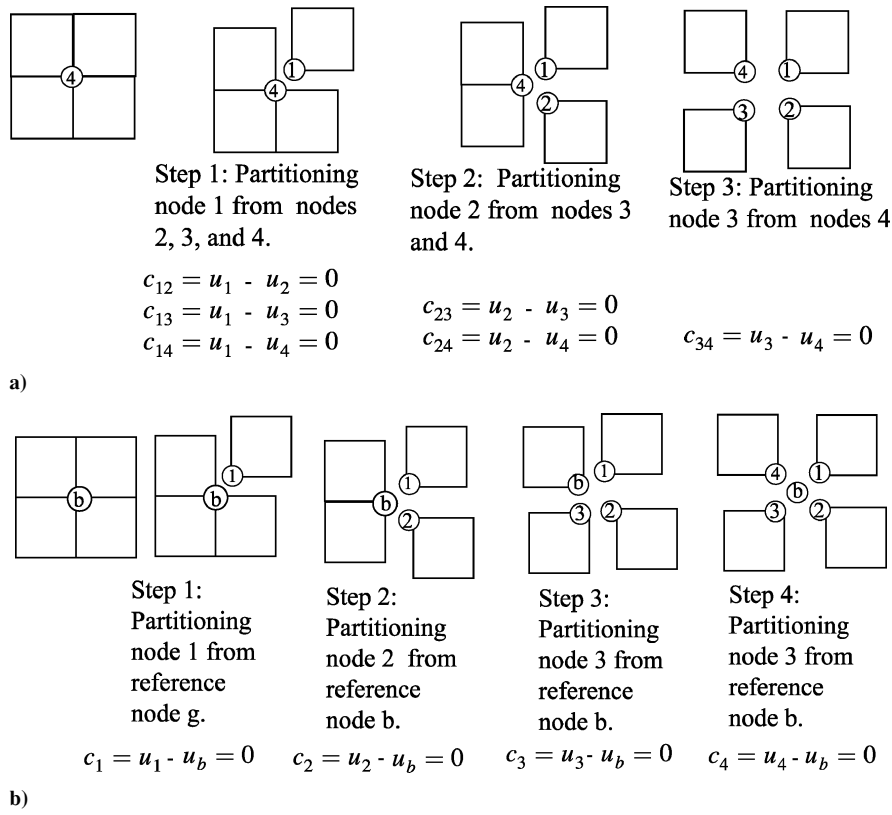


Fig. 2 Constraint conditions for the classical and localized  $\lambda$  methods: a) partitioning via classical Lagrange multipliers leads to nonunique choice of three constraint conditions out of six possible and b) partitioning via localized Lagrange multipliers leads to four unique constraint conditions.

because  $\Phi^T MR = 0$ . Similarly, if the damping matrix  $C$  is proportional, namely,

$$C = c_m M + c_k K \quad (8)$$

the same is true for the dissipative energy term,

$$\delta q^T \Phi^T CR \dot{\alpha} = \delta q^T \Phi^T CR \dot{\alpha} = 0 \quad (9)$$

The stationarity of  $\delta \Pi$  Eq. (6) thus yields the following matrix equation set:

$$\begin{bmatrix} \bar{K}_d & 0 & \Phi^T B & 0 \\ 0 & \bar{K}_\alpha & R_b^T & 0 \\ B^T \Phi & R_b & 0 & -L_b \\ 0 & 0 & -L_b^T & 0 \end{bmatrix} \begin{Bmatrix} q \\ \alpha \\ \lambda_\ell \\ u_b \end{Bmatrix} = \begin{Bmatrix} \Phi^T f \\ R^T f \\ 0 \\ 0 \end{Bmatrix}$$

$$\bar{K}_d = \Phi^T M \Phi D^2 + \Phi^T (CD + K) \Phi, \quad D = \frac{d}{dt}$$

$$\bar{K}_\alpha = R^T MR D^2 + R^T CR$$

$$R_b = B^T R, \quad L_b = B^T L \quad (10)$$

Here  $u_b$  is the assembled or global displacement vector along the partition boundary nodes.

A key element of the present four-field partitioned equations of motion is the inclusion of the generalized rigid-body coordinates  $\alpha$ . It is this feature that automatically takes care of each substructural self-equilibrium so that the distinction of determinate and indeterminate nature is obviated. It turns out that this feature also plays a fundamental role in the construction of a consistent flexibility-based component mode synthesis method to be discussed shortly. The pre-

ceding four-variable partitioned dynamic equation is the dynamic counterpart of the partitioned quasi-static equilibrium equation derived in Refs. 16 and 18 and has been used in the development of a parallel transient response analysis algorithm.<sup>19</sup>

### Formulation of Partitioned Eigenvalue Problem

Our aim is to approximate the spatially and modally partitioned equations of motion (10) by approximating some of the deformation modes  $\Phi$ . An excellent discussion of some of these procedures is offered by Spanos and Tsuha,<sup>10</sup> and a survey up to the late 1990s is offered in a text by Meirovitch.<sup>8</sup> As alluded to in the Introduction, because the principal objective of the present study is to develop a rational modal reduction/truncation procedure and scalable parallel computational algorithms for carrying out the component mode synthesis, we will carry out a general reduction process first. To this end, let us partition the deformation modes  $\Phi$  into two categories, the dominant substructural modes  $\Phi_d$  to be retained and the residual modes  $\Phi_r$  to be approximated as follows:

$$\Phi = \begin{bmatrix} \Phi_d & \Phi_r \\ (n \times m) & (n \times (n - m)) \end{bmatrix} \Rightarrow u = [R \quad \Phi_d \quad \Phi_r] \begin{Bmatrix} \alpha \\ q_d \\ q_r \end{Bmatrix} \quad (11)$$

Substituting this into Eq. (10), with  $C = 0$ , for the undamped case yields

$$\begin{bmatrix} \bar{\Lambda}_d & 0 & 0 & \Phi_d^T B & 0 \\ 0 & \bar{\Lambda}_r & 0 & \Phi_r^T B & 0 \\ 0 & 0 & I_\alpha D^2 & R_b^T & 0 \\ B^T \Phi_d & B^T \Phi_r & R_b & 0 & -L_b \\ 0 & 0 & 0 & -L_b^T & 0 \end{bmatrix} \begin{Bmatrix} q_d \\ q_r \\ \alpha \\ \lambda_\ell \\ u_b \end{Bmatrix} = \begin{Bmatrix} \Phi_d^T f \\ \Phi_r^T f \\ R^T f \\ 0 \\ 0 \end{Bmatrix}$$

$$\bar{\Lambda}_d = (\Lambda_d + I_d D^2), \quad \bar{\Lambda}_r = (\Lambda_r + I_r D^2) \quad (12)$$

in which we have employed the substructure-by-substructure eigenproblem result,

$$\mathbf{K} \begin{bmatrix} \Phi_d & \Phi_r \end{bmatrix} = \mathbf{M} \begin{bmatrix} \Phi_d & \Phi_r \end{bmatrix} \begin{bmatrix} \Lambda_d(m \times m) & \mathbf{0} \\ \mathbf{0} & \Lambda_r(N - m \times N - m) \end{bmatrix} \quad (13)$$

$\Lambda_d = \text{diag}\{(\omega_d)_1^2, (\omega_d)_2^2, \dots, (\omega_d)_m^2\}$ , etc.

A key focus of the present derivation is to eliminate the DOF of the higher modal components ( $\Phi_r, \Lambda_r$ ) instead of truncating them from the preceding equation. In so doing, we present several formulations.

**( $q_d, \alpha, \lambda_\ell, u_b$ ) Formulation**

In this formulation, we solve for the modal coordinate of the residual mode  $q_r$  from the second row of Eq. (12):

$$q_r = (\Lambda_r + \mathbf{I}_r D^2)^{-1} \Phi_r^T (f - \mathbf{B} \lambda_\ell) \quad (14)$$

Substituting this to eliminate  $q_r$  in Eq. (12) results in

$$\begin{bmatrix} \bar{\Lambda}_d & \mathbf{0} & \Phi_{db}^T & \mathbf{0} \\ \mathbf{0} & \mathbf{I}_\alpha D^2 & \mathbf{R}_b^T & \mathbf{0} \\ \Phi_{db} & \mathbf{R}_b & -\bar{\mathbf{F}}_{rb} & -\mathbf{L}_b \\ \mathbf{0} & \mathbf{0} & -\mathbf{L}_b^T & \mathbf{0} \end{bmatrix} \begin{bmatrix} q_d \\ \alpha \\ \lambda_\ell \\ u_b \end{bmatrix} = \begin{bmatrix} \Phi_d^T f \\ \mathbf{R}^T f \\ \mathbf{B}^T \bar{\mathbf{F}}_r f \\ \mathbf{0} \end{bmatrix}$$

$$\Phi_{db} = \mathbf{B}^T \Phi_d, \quad \bar{\mathbf{F}}_{rb} = \mathbf{B}^T \bar{\mathbf{F}}_r \mathbf{B}, \quad \bar{\mathbf{F}}_r = \Phi_r (\Lambda_r + \mathbf{I}_r D^2)^{-1} \Phi_r^T \quad (15)$$

Note that no approximation has been introduced in the preceding equation. Notice that  $\Phi_{db}$  represents the free-free substructural mode shapes along the partition-interface boundaries. Therefore, it is distinctly different from the so-called the interface constraint mode shapes employed in most existing component mode syntheses. The partitioned eigenvalue problem is obtained by invoking

$$D = -\omega^2, \quad f = \mathbf{0} \quad (16)$$

as given by

$$\begin{bmatrix} \bar{\Lambda}_d & \mathbf{0} & \Phi_{db}^T & \mathbf{0} \\ \mathbf{0} & -\omega^2 \mathbf{I}_\alpha & \mathbf{R}_b^T & \mathbf{0} \\ \Phi_{db} & \mathbf{R}_b & -\bar{\mathbf{F}}_{rb} & -\mathbf{L}_b \\ \mathbf{0} & \mathbf{0} & -\mathbf{L}_b^T & \mathbf{0} \end{bmatrix} \begin{bmatrix} q_d \\ \alpha \\ \lambda_\ell \\ u_b \end{bmatrix} = \begin{bmatrix} \mathbf{0} \\ \mathbf{0} \\ \mathbf{0} \\ \mathbf{0} \end{bmatrix}$$

$$\bar{\Lambda}_d = \Lambda_d - \omega^2 \mathbf{I}_d, \quad \bar{\mathbf{F}}_{rb} = \mathbf{B}^T \bar{\mathbf{F}}_r \mathbf{B}$$

$$\bar{\mathbf{F}}_r = \Phi_r (\Lambda_r - \omega^2 \mathbf{I}_r)^{-1} \Phi_r^T \quad (17)$$

The preceding partitioned eigenvalue problem equation (17), although exact, is impractical to solve via standard eigenvalue analysis procedures due to the transcendental nature of the dynamic interface flexibility  $\bar{\mathbf{F}}_{rb}$ . An approximation of the preceding formulation will be discussed later in this paper.

**( $q_d, \alpha, u_b$ ) Formulation**

If one further solves for  $\lambda_\ell$  from the third row of Eq. (17),

$$\lambda_\ell = (\bar{\mathbf{F}}_{rb})^{-1} [\Phi_{db} q_d + \mathbf{R}_b \alpha - \mathbf{L}_b u_b] \quad (18)$$

and substitutes this to eliminate  $\lambda_\ell$  in Eq. (17), the following equation results:

$$\begin{bmatrix} \bar{\Lambda}_d + \Phi_{db}^T \bar{\mathbf{F}}_{rb}^{-1} \Phi_{db} & \Phi_{db}^T \bar{\mathbf{F}}_{rb}^{-1} \mathbf{R}_b & -\Phi_{db}^T \bar{\mathbf{F}}_{rb}^{-1} \mathbf{L}_b \\ \mathbf{R}_b^T \bar{\mathbf{F}}_{rb}^{-1} \Phi_{db} & -\omega^2 \mathbf{I}_\alpha + \mathbf{R}_b^T \bar{\mathbf{F}}_{rb}^{-1} \mathbf{R}_b & -\mathbf{R}_b^T \bar{\mathbf{F}}_{rb}^{-1} \mathbf{L}_b \\ -\mathbf{L}_b^T \bar{\mathbf{F}}_{rb}^{-1} \Phi_{db} & -\mathbf{L}_b^T \bar{\mathbf{F}}_{rb}^{-1} \mathbf{R}_b & \mathbf{L}_b^T \bar{\mathbf{F}}_{rb}^{-1} \mathbf{L}_b \end{bmatrix} \begin{bmatrix} q_d \\ \alpha \\ u_b \end{bmatrix} = \begin{bmatrix} \mathbf{0} \\ \mathbf{0} \\ \mathbf{0} \end{bmatrix}, \quad \bar{\Lambda}_d = (\Lambda_d - \omega^2 \mathbf{I}_d) \quad (19)$$

Observe that  $\bar{\mathbf{F}}_r$  in Eq. (17) can be considered a dynamic residual flexibility, which plays a key role in the subsequent derivation. This is because the higher residual modes  $\Lambda_r$  and  $\Phi_r$ , are not directly computed; instead, they are approximated in terms of lower modes and substructural matrices. Hence, the fidelity of a component mode synthesis crucially depends on how the higher modes are approximated. The reason why  $\bar{\mathbf{F}}_r$  is physically a dynamic residual flexibility can be seen from the following identity:

$$\bar{\mathbf{F}}_r = [\mathbf{K} - \omega^2 \mathbf{M}]^{-1} - \{\Phi_d\} [\Lambda_d - \omega^2 \mathbf{I}_d]^{-1} \{\Phi_d^T\} - \mathbf{R} (-\omega^2 \mathbf{I}_\alpha)^{-1} \mathbf{R}^T \quad (20)$$

because  $[\mathbf{K} - \omega^2 \mathbf{M}]^{-1}$  can be expressed as

$$[\mathbf{K} - \omega^2 \mathbf{M}]^{-1} = \Phi \begin{bmatrix} (-\omega^2 \mathbf{I}_\alpha)^{-1} & \mathbf{0} & \mathbf{0} \\ \mathbf{0} & (\Lambda_d - \omega^2 \mathbf{I}_d)^{-1} & \mathbf{0} \\ \mathbf{0} & \mathbf{0} & (\Lambda_r - \omega^2 \mathbf{I}_r)^{-1} \end{bmatrix} \Phi^T$$

$$\Phi = [\mathbf{R}^T \quad \Phi_d^T \quad \Phi_r^T]^T \quad (21)$$

Using the preceding relations, the residual dynamic flexibility at the interfaces (or interface residual flexibility),  $\bar{\mathbf{F}}_{rb}$ , is given by

$$\bar{\mathbf{F}}_{rb} = \bar{\mathbf{F}}_{bb} - \Phi_{db} (\Lambda_d - \omega^2 \mathbf{I}_d)^{-1} \Phi_{db}^T - \mathbf{R}_b (-\omega^2 \mathbf{I}_\alpha)^{-1} \mathbf{R}_b^T$$

$$\bar{\mathbf{F}}_{bb} = \mathbf{B}^T [\mathbf{K} - \omega^2 \mathbf{M}]^{-1} \mathbf{B} \quad (22)$$

where  $\bar{\mathbf{F}}_{bb}$  is called the substructural interface flexibility.

**General Comments on the Present Partitioned Eigenanalysis Equations**

Before we begin to approximate the formulations derived in the preceding subsections, it is worth making several observations. First, the displacement-based formulation given by Eq. (19) consists of full matrix profile inasmuch as the inverse of the interface residual flexibility,  $\bar{\mathbf{F}}_{rb}^{-1}$ , appears in every submatrices. In contrast, the mixed formulation given by Eq. (15) involves the interface residual flexibility  $\bar{\mathbf{F}}_{rb}$  appears only once in its matrix profile.

Second, common to the two formulations is that, all of the matrix quantities are local substructural attributes except the ones involving the interface assembly Boolean matrix  $\mathbf{L}_b$ . Specifically, both the interface residual flexibility and the interface residual stiffness matrices are completely localized.

Third, the substructural rigid-body modes  $\mathbf{R}$  can be easily obtained by a geometrical consideration instead of resorting to eigenanalysis. In addition, because the substructural deformational modes  $\Phi_d$  are either free-free or with imposed boundary conditions for each substructure, experimentally determined modes and mode shapes can be readily used whenever deemed advantageous either due to analytical modeling difficulty or other experimental considerations. In other words, the present formulation is amenable to model validation.

Fourth, although not reported herein, two additional formulations have been derived, which illustrates that the four-variable partitioned formulation (12) can serve as a general framework for potentially new methods. We now proceed to approximating the two partitioned formulations to make their approximate formulas computationally tractable.

**Component Mode Synthesis Based on Interface Residual Flexibility Approximation**

Note that Eq. (17) has not introduced any approximation. To render the eigensolution problem using Eq. (17) into a computationally tractable form, we approximate the dynamic interface residual flexibility  $\bar{\mathbf{F}}_{rb}$  as follows. Under the assumption that the maximum interesting global frequency  $(\omega_g)_{\max}$  is smaller than the smallest natural frequency of the residual modes  $(\omega_r)_{\min}$ , that is,  $(\omega_g)_{\max} \ll (\omega_r)_{\min}$ ,

the transcendental dynamic interface residual flexibility  $\bar{F}_{rb}$  can be expanded as

$$\begin{aligned}\bar{F}_{rb} &= \Phi_{rb}(\Lambda_r - \omega^2 I_r)^{-1} \Phi_{rb}^T \\ &\approx \Phi_{rb} \Lambda_r^{-1} \Phi_{rb}^T + \omega^2 \Phi_{rb} \Lambda_r^{-2} \Phi_{rb}^T = \mathcal{F}_{rs} + \omega^2 \mathcal{F}_{rm}\end{aligned}\quad (23)$$

The static part  $\mathcal{F}_{rs}$ , so called the static interface residual flexibility, and the dynamic part  $\mathcal{F}_{rm}$  in Eq. (23) can be obtained indirectly from the mass and stiffness matrices of the system and the modal properties of the lower retained modes utilizing the mass orthogonality of the eigenvectors in Eq. (5) as derived in the Appendix as

$$\begin{aligned}\mathcal{F}_{rs} &= F_{bb} - \Phi_{db} \Lambda_d^{-1} \Phi_{db}^T \\ F_{bb} &= B^T M^{-\frac{1}{2}} [M^{-\frac{1}{2}} K M^{-\frac{1}{2}}]^+ M^{-\frac{1}{2}} B \\ \mathcal{F}_{rm} &= B^T M^{-\frac{1}{2}} ([M^{-\frac{1}{2}} K M^{-\frac{1}{2}}])^2 M^{-\frac{1}{2}} B - \Phi_{db} \Lambda_d^{-2} \Phi_{db}^T\end{aligned}\quad (24)$$

Substituting Eqs. (23) and (24) into the  $(q_d, \alpha, \lambda_\ell, u_b)$ -formulation Eq. (17), we arrive at the following tractable component mode synthesis:

$$A_f \Phi_f = \omega^2 B_f \Phi_f \quad (25)$$

$A_f$ ,  $B_f$ , and  $\Phi_f$  in Eq. (25) are given by

$$\begin{aligned}A_f &= \begin{bmatrix} \Lambda_d & \Phi_{db}^T & \mathbf{0} & \mathbf{0} \\ \Phi_{db} & -\mathcal{F}_{rs} & R_b & -L_b \\ \mathbf{0} & R_b^T & \mathbf{0} & \mathbf{0} \\ \mathbf{0} & -L_b^T & \mathbf{0} & \mathbf{0} \end{bmatrix}, \quad B_f = \begin{bmatrix} I_d & \mathbf{0} & \mathbf{0} & \mathbf{0} \\ \mathbf{0} & \mathcal{F}_{rm} & \mathbf{0} & \mathbf{0} \\ \mathbf{0} & \mathbf{0} & I_\alpha & \mathbf{0} \\ \mathbf{0} & \mathbf{0} & \mathbf{0} & \mathbf{0} \end{bmatrix} \\ \Phi_f &= [\Phi_q^T \quad \Phi_\lambda^T \quad \Phi_\alpha^T \quad \Phi_u^T]^T\end{aligned}\quad (26)$$

Once the partitioned eigenvalue problem is solved, the global mode shapes are computed according to

$$\Phi_g = [\Phi_d \Phi_q + R \Phi_\alpha - \bar{F}_r B \Phi_\lambda] \quad (27)$$

*Remark:* The static interface residual flexibility  $\mathcal{F}_{rs}$  given in Eq. (24) may be used as a substructural modal selection guide. To see this, recall  $\mathcal{F}_{rs}$  as

$$\mathcal{F}_{rs}|_{k=1}^{N_d} \equiv F_{bb} - \sum_{k=1}^{N_d} (\Phi_{db})_k (\omega_d^2)_k^{-1} (\Phi_{db})_k^T \quad (28)$$

where  $N_d$  is the number of modes selected for each substructure. Note that the interface flexibility (not interface residual flexibility)  $F_{bb}$  remains fixed for each partitioned substructure. Hence, one can assess the changes in the norm of the static interface residual flexibility  $\mathcal{F}_{rs}$  for each addition or deletion of the retained modal contribution  $(\Phi_{db})_k$ . This observation enables us to rank those modes that minimizes the norm of the interface residual flexibility and retain them, thus, providing a rational substructural mode selection criterion. For example, a possible substructural modal truncation criterion may utilize  $\epsilon_{cum}$  for the cumulative mode selection criterion as

$$\epsilon_{cum} = 1 - \|\mathcal{F}_{rs}|_{k=1}^{N_d}\| / \|F_{bb}\| \quad (29)$$

for each substructure, where  $\epsilon_{cum}$  is the desired mode cutoff tolerance. The error criterion  $\epsilon_{cum}$  is defined by the summation of the contributions of a group of modes to the interface flexibility. We can access the contribution of individual modes mode-by-mode or substructure-by-substructure with an individual modal truncation

criterion  $\epsilon_{ind}$ . For example, the modal selection criterion for the  $k$ th mode can be

$$\begin{aligned}\epsilon_{ind} &= 1 - \|\mathcal{F}_{rs}|_k\| / \|F_{bb}\| \\ \mathcal{F}_{rs}|_k &\equiv F_{bb} - (\Phi_{db})_k (\omega_d^2)_k^{-1} (\Phi_{db})_k^T\end{aligned}\quad (30)$$

The modal selection criteria  $\epsilon_{cum}$  and  $\epsilon_{ind}$  have values between 0 and 1: 0 for the worst and 1 for the best modal selection for minimization of the interface residual flexibility.

### Component Mode Synthesis Based on Interface Residual Stiffness Approximation

To render the eigensolution problem using Eq. (19) into a computationally tractable form, we approximate the dynamic interface residual stiffness  $\bar{F}_{rb}^{-1}$  as follows. Under the same assumption that is applied in deriving the approximate flexibility  $[(\omega_g)_{max} \ll (\omega_f)_{min}]$ , the inverse of the dynamic interface residual flexibility  $\bar{F}_{rb}^{-1}$  in Eq. (17) can be expanded as

$$\bar{F}_{rb}^{-1} = \mathcal{F}_{rs}^{-1} - \omega^2 \mathcal{F}_{rs}^{-1} \mathcal{F}_{rm} \mathcal{F}_{rs}^{-1} = K_{rb} - \omega^2 M_{rb} \quad (31)$$

where  $M_{rb}$  is the dynamic part of the interface residual stiffness, which may be discarded because its omission would be equivalent to neglecting the dynamic part of the residual flexibility matrix  $\mathcal{F}_{rm}$ . Substituting the approximation of Eq. (31) into the  $(q_\ell, \alpha, u_{gb})$ -formulation equation (19) leads to the following approximate formula:

$$A_s \Phi_s = \omega^2 B_s \Phi_s \quad (32)$$

Here  $A$ ,  $B_s$ , and  $\Phi_s$  are given by

$$\begin{aligned}A_s &= \begin{bmatrix} (\Lambda_d + \Phi_{db}^T K_{rb} \Phi_{db}) & \Phi_{db}^T K_{rb} R_b & -\Phi_{db}^T K_{rb} L_b \\ R_b^T K_{rb} \Phi_{db} & R_b^T K_{rb} R_b & -R_b^T K_{rb} S L_b \\ -L_b^T K_{rb} \Phi_{db} & -L_b^T K_{rb} R_b & L_b^T K_{rb} L_b \end{bmatrix} \\ B_s &= \begin{bmatrix} (I_d + \Phi_{db}^T M_{rb} \Phi_{db}) & \Phi_{db}^T M_{rb} R_b & -\Phi_{db}^T M_{rb} L_b \\ R_b^T M_{rb} \Phi_{db} & (I_\alpha + R_b^T M_{rb} R_b) & -R_b^T M_{rb} L_b \\ -L_b^T M_{rb} \Phi_{db} & -L_b^T M_{rb} R_b & L_b^T M_{rb} L_b \end{bmatrix} \\ \Phi_s &= [\Phi_q^T \quad \Phi_\alpha^T \quad \Phi_u^T]^T\end{aligned}\quad (33)$$

In approximating  $\bar{F}_{rb}$ , one performs matrix approximation only once. However, to obtain approximations of the dynamic interface residual stiffness  $\bar{F}_{rb}^{-1}$ , one must carry out two matrix approximations.

### Craig-Bampton Method

The Craig-Bampton component mode synthesis method<sup>2</sup> can be expressed in terms of the present nomenclature as

$$\begin{aligned}\begin{bmatrix} \Lambda_i & \mathbf{0} \\ \mathbf{0} & L_b^T K_{bb}^S L_b \end{bmatrix} \begin{Bmatrix} q_i \\ u_b \end{Bmatrix} &= \omega^2 \begin{bmatrix} I_{i\ell} & \Phi_i^T \tilde{M}_{ib} L_b \\ L_b^T \tilde{M}_{bi} \Phi_{i\ell} & L_b^T M_{bb}^S L_b \end{bmatrix} \begin{Bmatrix} q_i \\ u_b \end{Bmatrix} \\ K_{bb}^S &= (K_{bb} - K_{bi} K_{ii}^{-1} K_{ib}) \\ M_{bb}^S &= M_{bb} + K_{bi} K_{ii}^{-1} M_{ii} K_{ii}^{-1} K_{ib} - M_{bi} K_{ii}^{-1} K_{ib} - K_{bi} K_{ii}^{-1} M_{ib} \\ \tilde{M}_{ib} &= M_{ib} - M_{ii} K_{ii}^{-1} K_{ib}\end{aligned}\quad (34)$$

in which  $M_{bb}$  and  $K_{bb}$  are the substructural boundary attributes,  $M_{bi}$  and  $K_{bi}$  are the coupling matrices between the substructural interior and the substructural boundary attributes, and the so-called normal mode pairs  $(\Lambda_i, \Phi_i)$  are obtained by the eigenproblem for each substructure,

$$K_{ii} \Phi_i = M_{ii} \Phi_i \Lambda_i \quad (35)$$

where the subscript  $i$  refers to the interior DOF for each substructure when the substructural interface DOF is completely fixed and the subscript  $b$  denotes the global interface DOF.

Because the Craig–Bampton method<sup>2</sup> is perhaps the most widely used mode synthesis method, it will be instructive to examine the differences between the present methods Eqs. (25) and (32) and the Craig–Bampton method given by Eq. (34). This is detailed in the next section.

### Theoretical Attributes of the Present Methods

The fundamental difference of the present component mode synthesis formulations in Eqs. (25) from the Craig–Bampton method is that the present method is flexibility based. Advances in the efficient computation of substructural flexibility<sup>16,20</sup> renders the flexibility-based component mode synthesis as competitive with a stiffness-based method. In that regard, the present flexibility-based component mode synthesis method equations (25) is akin to the MacNeal method.<sup>6</sup>

Second, the present method employs the free–free substructural modes, which is in contrast to the use of interior substructural modes by the Craig–Bampton method.<sup>2</sup> This means that all of the approximations in arriving at the flexibility-based methods in Eqs. (25) and (32) have been done on the localized dynamic interface residual flexibility  $\bar{F}_{rb}$  Eq. (22). On the other hand, the Craig–Bampton method Eq. (34) makes an approximation in linking the substructural interior modes to the boundary displacement; in other words, it links its local characteristics to the global DOF.

Third, from a practical viewpoint, the present substructural mode selection criterion derived in Eq. (29) is perhaps a novel attribute, whose robustness will be evaluated in the “Numerical Experiments” section.

Finally, the solution of the global eigenvalue problem is completely parallelizable. This can be demonstrated as follows. Consider the following iteration for generating either Lanczos or subspace vector

$$\bar{A}_f x^{k+1} = \bar{B}_f x^k = b^k$$

$$x = \begin{Bmatrix} q_d \\ q_\lambda \\ \alpha \\ u_{gb} \end{Bmatrix}, \quad b^k = \bar{B}_f x^k = \begin{Bmatrix} b_1 \\ b_2 \\ b_3 \\ b_4 \end{Bmatrix} \quad (36)$$

for solving the eigenproblem equation (25). Because  $\Lambda_d$  is diagonal, we solve for  $q_d$ ,

$$q_d^{(k+1)} = \Lambda_d^{-1} (b_1^k - \Phi_{db} q_\lambda^{(k+1)}) \quad (37)$$

Substituting this into Eq. (25) yields the following arrow-headlike equation:

$$\begin{bmatrix} \mathcal{F}_b & -R_b & L_b \\ -R_b^T & 0 & 0 \\ L_b^T & 0 & 0 \end{bmatrix} \begin{Bmatrix} q_\lambda \\ \alpha \\ u_b \end{Bmatrix}^{(k+1)} = \begin{Bmatrix} \Phi_{db} \Lambda_d^{-1} b_1 - b_2 \\ b_3 \\ 0 \end{Bmatrix}^k \quad (38)$$

**Q6** Equation (38) is well suited to parallel computations.<sup>14,19</sup>

### Numerical Experiments

We have implemented both the flexibility-based component mode method (25) and the stiffness-based component mode synthesis method (32), as well as the Craig–Bampton<sup>2</sup> method for comparison purposes.

#### Plate Vibration Modeled by Two Substructures

The first example is a clamped plate as shown in Fig. 3, which Craig and Bampton<sup>2</sup> reported in their original paper. Substructure 1 consists of 162 DOF and that of substructure 2 of 90 DOF. The interface consists of 18 DOF. For the present component mode synthesis, 10 substructural modes from each substructure are retained. Thus, the total generalized coordinates plus the interface DOF consists of 38 DOF.

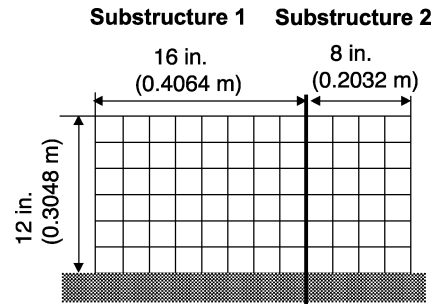


Fig. 3 Layout of cantilever plate partitioned into two substructures.

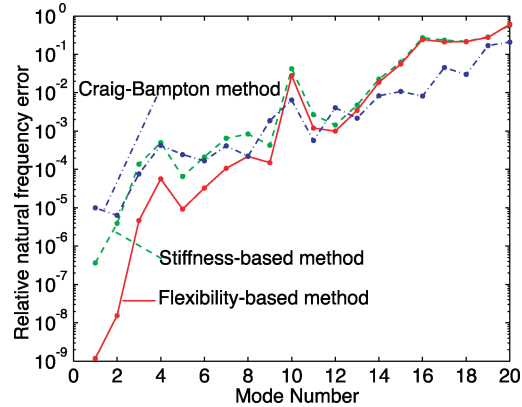


Fig. 4 Relative errors in CSM computed natural frequencies for the fixed plate.

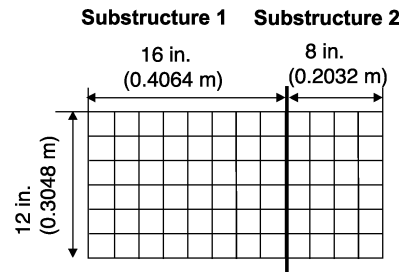


Fig. 5 Layout of free–free plate partitioned into two substructures.

Figure 4 shows the errors in the natural frequencies computed using the present two component mode synthesis (CMS) methods compared to the full-system eigenvalues. Observe that the CMS synthesis based on the present flexibility-based method (25) outperforms both the present stiffness-based method and the Craig–Bampton method<sup>2</sup> up to the first nine global modes. In fact, for the first lowest mode the accuracy of the flexibility-based method yields about three to four digits of accuracy improvements over the Craig–Bampton method.

The second example is a free–free plate vibration, as shown in Fig. 5, by removing the clamped boundary condition from the first example. For both substructures 1 and 2, the first 10 modes are selected as in the clamped plate case. Thus, the total generalized coordinates plus the interface global displacements consist of 41 DOF. In practice, one should include more substructural modes for free–free plate vibrations because any of the intrinsic modes is free to vibrate; for the present experiment the same number modes are used as in the clamped case.

Figure 6 shows the errors incurred in the CMS-generated global eigenvalues compared with the full-system free–free plate vibration. Observe that the error in the first nonzero mode computed by the present flexibility-based method equation (25) for this free–free plate is about  $10^{-4}$ , whereas that of the clamped plate is about  $10^{-7}$ . This clearly indicates that one needs more substructural modes for the free–free plate vibrations than for the clamped case. Because the first three modes are rigid-body modes of the complete system,

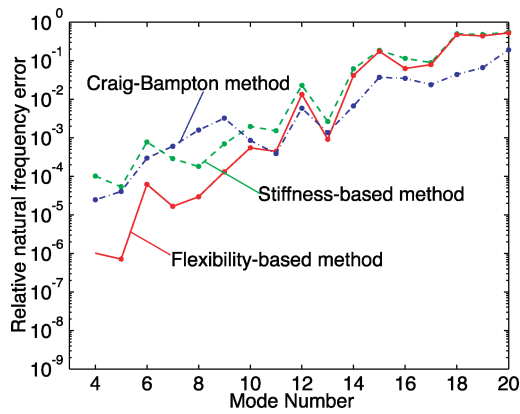


Fig. 6 Relative errors in CSM computed natural frequencies for the free-free plate vs substructural modes retained.

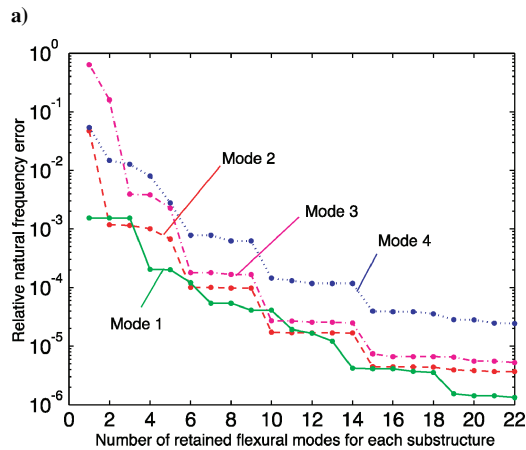
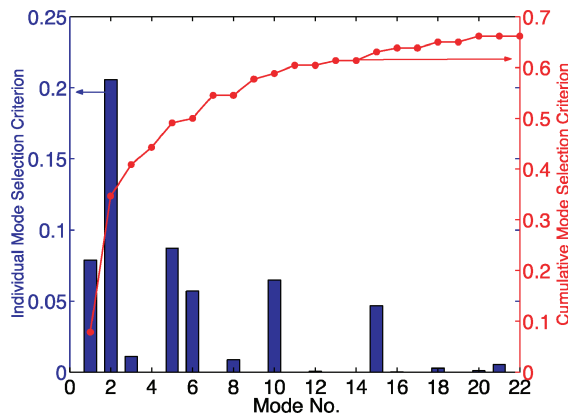


Fig. 7 Performance of the model selection criteria: a) cumulative mode selection criterion vs the number of modes retained and individual mode selection criterion vs each mode for free-free plate problem and b) relative natural frequency errors of first four modes of free-free plate problem vs substructural modes retained.

the first non-zero modes are in fact the fourth mode. Note once again that the present flexibility-based method yields substantially improved accuracy over the Craig-Bampton method, as well as the present residual stiffness method (32).

Because the flexibility-based method (25) appears to show promise in terms of accuracy and its adaptability to efficient parallel implementation, the substructural mode selection criteria (29) and (30) are evaluated using the free-free vibration problem. Note that the present two mode selection criteria do not utilize any loading function characteristics. Figures 7a shows the performance of the present mode selection criteria vs the number of substructural modes included. The upper curve indicates the cumulated weight of each mode on the overall mode-by-mode energy contribution,

whereas the bottom bar-formatted part shows the extent of their contribution in terms of the global natural frequency error vs. the number of modes retained. The larger the value of the individual modal selection index is, the more significant that particular number of substructural modes to be included. As can be seen, although not conclusive, they do offer satisfactory indications providing which modes are to be retained and how many modes are to be retained.

### Three-Dimensional Ring

Encouraged by the performance of the present flexibility-based method for simple plates, we applied the present method to a ring modeled by three-dimensional elements consisting of 16 substructures with 166,320 total global DOF provided by Garth Reese of Sandia National Laboratories.

Table 1 and Fig. 8 show both the 16 substructures and the substructural DOF for each substructure, with 184,017 total substructural DOF, whereas there 35,394 total interface are DOF. Hence, the partitioned DOF is about 5.2 times the interface DOF.

To gain insight into how the number of interface modes retained would affect the overall eigenvalue accuracy, 20 substructural modes are retained for each substructure and the interface modes are varied from 50, to 100, to 150 for each interface. The case of 200 interface

Table 1 Free-free ring modeled by solid elements

Substructural number	Total DOF	Interface DOF
<i>Partitioned structures</i>		
1	14,403	2,256
2	11,070	2,151
3	11,061	2,142
4	11,097	2,238
5	11,088	2,256
6	14,463	2,265
7	11,097	2,247
8	11,097	2,265
9	11,106	2,274
10	11,070	2,151
11	11,061	2,142
12	11,097	2,238
13	11,079	2,238
14	11,097	2,238
15	11,061	2,142
16	11,070	2,151
<i>Assembled structures</i>		
	166,320	17,697



Fig. 8 Free-free ring modeled by solid elements.

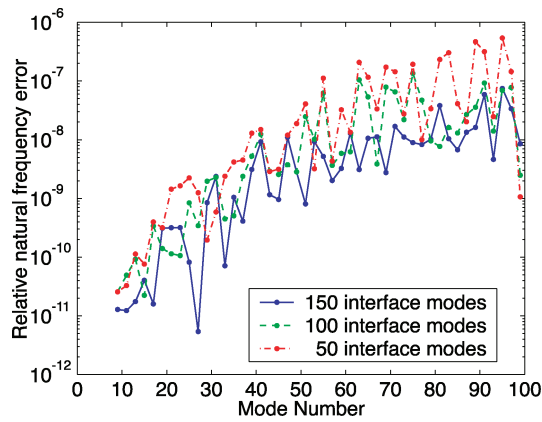


Fig. 9 Sensitivity of the number of interface modes to natural frequency error; relative natural frequency errors vs global structural modes.

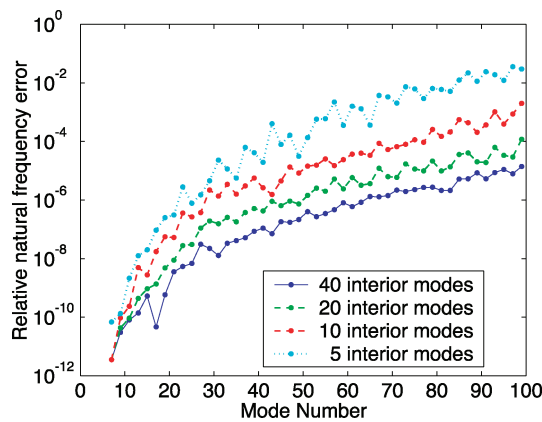


Fig. 10 Sensitivity of the number of retained interior modes to natural frequency error for the flexibility-based method; relative natural frequency errors vs global structural modes.

was also carried out and showed no discernable difference from that of 150 interface modes. Figure 9 summarizes the result, which shows that the most one could improve the accuracy from 50 to 150 interface modes is less than one digit improvement. Thus 50 interface modes are chosen in subsequent analysis with error range from  $10^{-11}$  to  $10^{-6}$  up to 100 global mode.

Next, the number of substructural modes is varied, as shown in Fig. 10. The results show that, as the number of substructural modes are increased from 5 to 40, the accuracy for intermediate modes (around 50th global modes) improved by more than three digits. The same sensitivity computations were also carried out for the stiffness-based method and the Craig–Bampton method and indicated both methods yielded an improvement in accuracy, up to about two digits.

Figure 11 summarizes the accuracy of the three methods when 20 normal modes and 50 interface modes are selected. Although not conclusive, the present flexibility-based method offers about four-digit accuracy improvement over the Craig–Bampton method for low modes and continues to offer better accuracy to 100 global modes. Note that the present stiffness-based method and the Craig–Bampton method yield about the same accuracy, which reconfirms the accepted notion: There is little room to improve beyond the Craig–Bampton method among stiffness-based methods. Figure 12 shows the convergence behavior of the three methods: the relative natural frequency errors of the 50th mode computed by the three methods vs the number of modes retained. This shows that the flexibility-based method converges faster than the Craig–Bampton and the present stiffness-based methods as the number of retained modes increases.

#### Evaluation of Present Substructural Mode Selection Criteria

To evaluate the proposed substructural mode selection criteria (29) and (30), we have plotted the individual (mode-by-mode

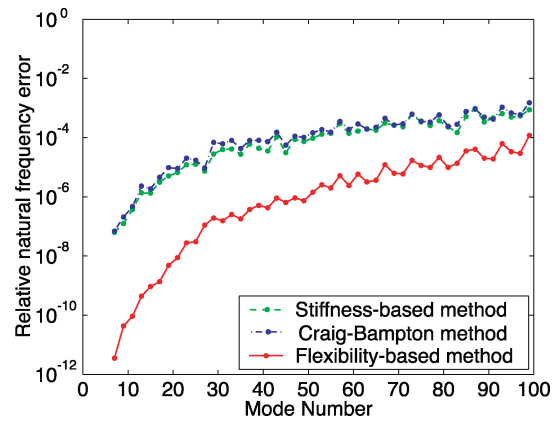


Fig. 11 Relative errors in CSM computed natural frequencies of the present stiffness-based method, flexibility-based method, and Craig–Bampton method vs the number of modes retained. All natural frequencies calculated using 20 interior modes for each substructure.

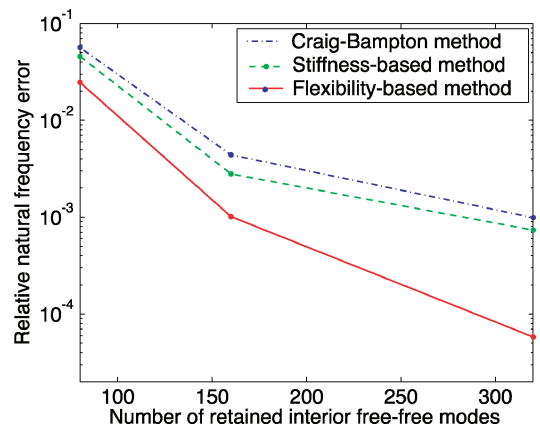


Fig. 12 Relative error of the 50th mode computed by the present stiffness-based method, flexibility-based method, and Craig–Bampton method vs the number of modes retained; all natural frequencies calculated using 20 interior modes for each substructure.

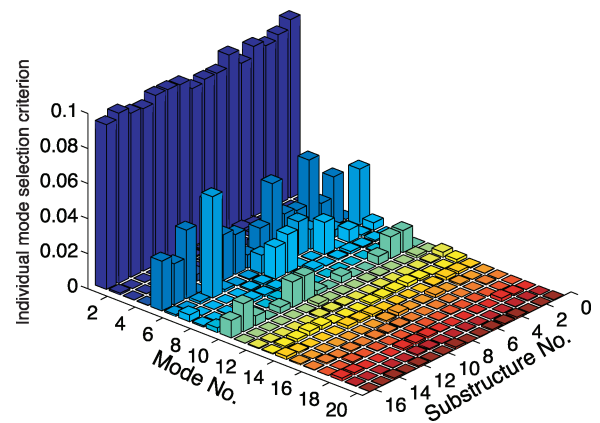


Fig. 13 Individual mode selection criteria for each mode of 16 substructures.

norm and substructure-by-substructure) model selection criterion in Fig. 13, which indicates that some particular modes make a large contribution to the accuracy of eigenvalue problem. Figure 14a, which sums up all of the substructural attributes to get the mode-by-mode cumulative as well as individual model selection criteria, shows how many of retained modes are adequate.

To verify whether the present substructural mode selection criteria provide a dependable indication, the actual global mode-by-mode accuracy vs the number of substructural modes retained is plotted for the first 10 global modes in Fig. 14b. By comparing Figs. 13 and 14,

**Table 2 Comparison of computational effort**

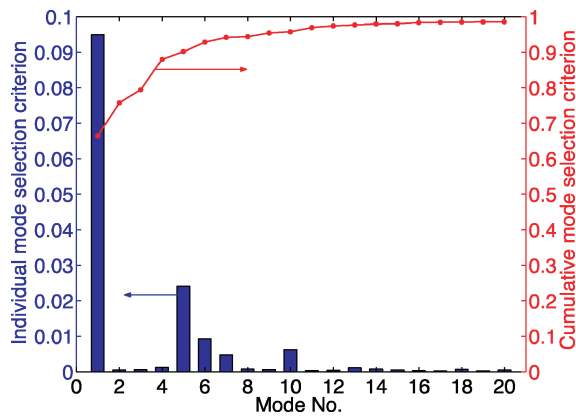
Computation	Present flexibility-based method	Craig–Bampton (CB) method
Substructural eigenanalysis <sup>a</sup> (100 modes)	711 <sup>b</sup>	415
Forming Schur complement for CB method, $\mathcal{F}_{rs}$ , $\mathcal{F}_{rm}$ for flexibility-based method <sup>c</sup>	135	139
Computing interface modes (250 modes) <sup>d</sup>	302	369
Factorization for generating global eigenanalysis vector	117	88
Global eigenanalysis (50 interface modes for each interface, and 20 modes for each substructure)	0.62	0.95

<sup>a</sup>Present flexibility-based method utilize all DOF in each substructure, whereas CB method employs only interior attributes.

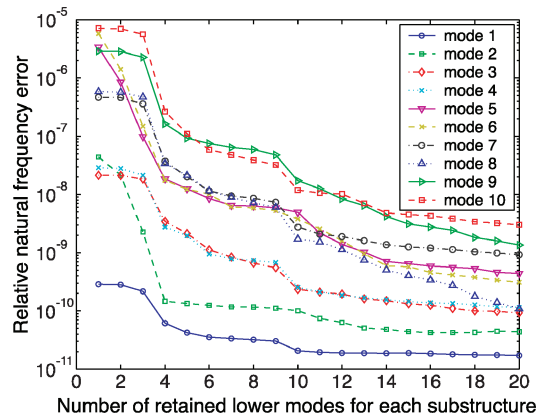
<sup>b</sup>Relative computing time (seconds) on typical engineering work station; for this example, a Dell dual process machine.

<sup>c</sup>In practice, Schur complement formation in CB method must conform to the tree-structure invoked; on the other hand, present method is hierarchy-free formation.

<sup>d</sup>The reduction of interface modes in CB method not fully parallelizable; fully parallelizable for the present method.



a) Mode selection criteria



b) Relative natural frequency errors

**Fig. 14 Performance of the model selection criteria: a) cumulative mode selection criteria vs number of mode retained and individual mode selection criteria vs each mode for free–free plate problem and b) relative natural frequency errors of first 10 modes of the ring problem vs substructural modes retained.**

one concludes that the present substructural mode selection criteria (29) and (30) indeed appear to offer a dependable selection guide.

**Computational Comparison**

Finally, the computational effort in the MATLAB<sup>®</sup> computing environment is summarized in Table 2. Clearly, the present flexibility-based method requires more computational effort in generating substructural modes than the Craig–Bampton method be-

cause it involves the entire substructural models. However, the present flexibility-based method is amenable to a scalable computing algorithms as shown in Eq. (38). This scalability potential may outweigh the increased computational overhead in computing free–free substructural eigenvalue analysis.

**Summary**

A family of exact transcendental eigenproblem equations have been derived from the four-variable partitioned equations of motion for linear structure equation (10). The exact transcendental equations (15) and (19) are then approximated to yield computationally tractable eigenproblem: a flexibility-based method (25) and a stiffness-based method (32). By the examination of the invoked approximations two substructural mode selection criteria are derived in Eqs. (29) and (30). Several theoretical attributes of the present methods are offered for the readers who are familiar with the Craig–Bampton method equation (34).

Note that an essential difference between the present flexibility-based component mode synthesis methods equation (25) vs the Craig–Bampton method equation (34) is that, whereas the present method involves the presence of substructural rigid-body modes, the Craig–Bampton method does not, which has been shown to be advantageous in parallel/parallel computations. This is because the rigid-body modes are the fundamental motions that satisfy self-equilibrium of each floating substructure. The absence of substructural rigid-body modes and their generalized coordinates may, perhaps, hinder a partitioned/parallel version of the Craig–Bampton method from achieving scalability, as may be observed in one of its possible parallel implementations.<sup>21</sup>

The flexibility-based mode synthesis method (25) developed has been implemented and evaluated for performance along with the present stiffness-based method (32) and the Craig–Bampton method. Applications to simple plate problem and one moderate-size ring problem indicate that the present flexibility-based method yields substantially improved accuracy over the Craig–Bampton method, especially for low-frequency modes. In particular, the substructural mode selection criterion developed as part of the derivation appears to be robust and provides a dependable cumulative selection guide.

Although not validated, the present methods can be implemented efficiently in a parallel computer because the eigensolution iterations can exploit the arrowlike matrix equation (38), which is known for its scalability when implemented in parallel computers. We elaborate this aspect further: First, large-scale eigenvalue analysis using component mode synthesis methods presently suffer from their rapid accuracy degradation for materially and/or geometrically heterogeneous structures. The use of localized Lagrange multipliers (see Ref. 17) may be applied to the regularization of heterogeneity, leading to substantial accuracy improvements. Second, the present methods employs the free–free substructural rigid-body modes as its fundamental modes, which are present in the arrow-headlike matrix equation (38). This is in contrast to existing structural parallel software wherein the substructural rigid-body modes are retroactively added for the sake of improving the conjugate gradient iterations. Third, the present methods allows no redundancies in the interface Lagrange multipliers because the methods have been developed using the variationally complete partitioned formulation. Thus, they can exploit the parallel construct presented in Refs. 14 and 15.

**Appendix**

The mass, stiffness matrices, and the eigenproperties of the structural system satisfy the following orthogonality relations:

$$\Phi^T M \Phi = I, \quad \Phi^T K \Phi = \Lambda$$

$$\Lambda = \text{diag}(\mathbf{0}_\alpha, \Lambda_\ell, \Lambda_r), \quad \Phi = [R^T \quad \Phi_\ell^T \quad \Phi_r^T]^T \quad (A1)$$

Let  $\hat{\Phi}$  be the transformed eigenvectors,

$$\hat{\Phi} = M^{\frac{1}{2}} \Phi \quad (A2)$$

Q8

Q10

Q11

Q9

Q12

The orthogonality relations in Eq. (A1) can be rewritten according to the transformed eigenvectors as

$$\hat{\Phi}^T \hat{\Phi} = I \quad (A3)$$

$$\hat{\Phi}^T M^{-\frac{1}{2}} K M^{-\frac{1}{2}} \hat{\Phi} = \Lambda \quad (A4)$$

Note that  $\hat{\Phi}$  is a unitary matrix for the orthogonality in Eq. (A3). Thus, we can get the following relation from Eq. (A4):

$$M^{-\frac{1}{2}} K M^{-\frac{1}{2}} = \hat{\Phi} \Lambda \hat{\Phi}^T \quad (A5)$$

The generalized inverse of Eq. (A5) results in

$$\begin{aligned} [M^{-\frac{1}{2}} K M^{-\frac{1}{2}}]^+ &= [\hat{\Phi}_\ell \quad \hat{\Phi}_r] \begin{bmatrix} \Lambda_\ell^{-1} & \mathbf{0} \\ \mathbf{0} & \Lambda_r^{-1} \end{bmatrix} \begin{bmatrix} \hat{\Phi}_\ell \\ \hat{\Phi}_r \end{bmatrix} \\ &= \hat{\Phi}_\ell \Lambda_\ell^{-1} \hat{\Phi}_\ell^T + \hat{\Phi}_r \Lambda_r^{-1} \hat{\Phi}_r^T \end{aligned} \quad (A6)$$

From Eqs. (A2) and (A6), we can get the desired expression

$$\begin{aligned} \mathcal{F}_{rs} &= B^T \Phi_r \Lambda_r^{-1} \Phi_r^T B \\ &= B^T M^{-\frac{1}{2}} [M^{-\frac{1}{2}} K M^{-\frac{1}{2}}]^+ M^{-\frac{1}{2}} B - \Phi_{\ell b} \Lambda_\ell^{-1} \Phi_{\ell b}^T \end{aligned} \quad (A7)$$

The square of Eq. (A6) provided with the orthogonality in Eq. (A3) yields

$$\begin{aligned} ([M^{-\frac{1}{2}} K M^{-\frac{1}{2}}]^+)^2 &= [\hat{\Phi}_\ell \quad \hat{\Phi}_r] \begin{bmatrix} \Lambda_\ell^{-2} & \mathbf{0} \\ \mathbf{0} & \Lambda_r^{-2} \end{bmatrix} \begin{bmatrix} \hat{\Phi}_\ell \\ \hat{\Phi}_r \end{bmatrix} \\ &= \hat{\Phi}_\ell \Lambda_\ell^{-2} \hat{\Phi}_\ell^T + \hat{\Phi}_r \Lambda_r^{-2} \hat{\Phi}_r^T \end{aligned} \quad (A8)$$

From Eqs. (A2) and (A8), we can get the desired expression as

$$\begin{aligned} \mathcal{F}_{rm} &= B^T \Phi_r \Lambda_r^{-2} \Phi_r^T B \\ &= B^T M^{-\frac{1}{2}} ([M^{-\frac{1}{2}} K M^{-\frac{1}{2}}]^+)^2 M^{-\frac{1}{2}} B - \Phi_{\ell b} \Lambda_\ell^{-2} \Phi_{\ell b}^T \end{aligned} \quad (A9)$$

### Acknowledgments

This research has been supported by Lawrence Livermore National Laboratory (Contract B347880), National Science Foundation (Grants ECS-9725504 and CMS-0219422), and by a post-doctoral fellowship from the Korea Science and Engineering Foundation.

### References

<sup>1</sup>Benfield, W. A., and Hrudá, R. F., "Vibration Analysis of Structures by Component Mode Substitution," *AIAA Journal*, Vol. 9, 1971, pp. 1255–1261.  
<sup>2</sup>Craig, R. R., Jr., and Bampton, M. C. C., "Coupling of Substructures for Dynamic Analysis," *AIAA Journal*, Vol. 6, 1968, pp. 1313–1319.  
<sup>3</sup>Craig, R. R., Jr., and Chang, C.-J., "On the Use of Attachment Modes in Substructure Coupling for Dynamic Analysis," *AIAA Paper 77-405*, 1977.

<sup>4</sup>Hintz, R. M., "Analytical Methods in Component Modal Synthesis," *AIAA Journal*, Vol. 13, 1975, pp. 1007–1016.  
<sup>5</sup>Hurty, W. C., "Dynamic Analysis of Structural Systems Using Component Modes," *AIAA Journal*, Vol. 3, 1965, pp. 678–685.  
<sup>6</sup>MacNeal, R. H., "A Hybrid Method of Component Mode Synthesis," *Comp. and Struct.*, Vol. 1, 1971, pp. 581–601. **Q14**  
<sup>7</sup>Meirovitch, L., and Hale, A. L., "On the Substructure Synthesis Method," *Vol. 19, No. 7*, 1981, pp. 940–947.  
<sup>8</sup>Meirovitch, L., *Principles and Techniques of Vibrations*, Prentice-Hall, New York, pp. 558–579. **Q15**  
<sup>9</sup>Rubin, S., "Improved Component-Mode Representation for Structural Dynamic Analysis," *AIAA Journal*, Vol. 13, 1975, pp. 995–1006.  
<sup>10</sup>Spanos, J. T., and Tsuha, W. S., "Selection of Component Modes for Flexible Multibody Simulation," *Journal of Guidance, Control, and Dynamics*, Vol. 14, No. 2, 1991, pp. 278–286.  
<sup>11</sup>Chen, P.-S., "Scalable Substructuring Methods for High Performance Structural Analysis," Ph.D. Dissertation, Dept. of Aerospace Engineering Sciences, Univ. of Colorado, Boulder, CO, 1997. **Q16**  
<sup>12</sup>Farhat, C., and Roux, F.-X., "A Method of Finite Element Tearing and Interconnecting and Its Parallel Solution Algorithm," *Int. J. of Numer. Mech. Eng.*, Vol. 32, pp. 1205–1227. **Q17**  
<sup>13</sup>Farhat, C., Chen, P.-S., Mandel, J., and Roux, F.-X., "The Two-Level FETI Method Part II: Extension to Shell Problems, Parallel Implementation and Performance Results," *Computer Methods in Applied Mechanics and Engineering*, Vol. 155, 1998, pp. 153–179.  
<sup>14</sup>Justino, M. R., Jr., Park, K. C., and Felippa, C. A., "An Algebraically Partitioned FETI Method for Parallel Structural Analysis: Implementation and Numerical Performance Evaluation," *International Journal of Numerical Methods in Engineering*, Vol. 40, 1997, pp. 2739–2758.  
<sup>15</sup>Park, K. C., Justino, M. R., Jr., and Felippa, C. A., "An Algebraically Partitioned FETI Method for Parallel Structural Analysis: Algorithm Description," *International Journal of Numerical Methods in Engineering*, Vol. 40, 1997, pp. 2717–2737.  
<sup>16</sup>Park, K. C., and Felippa, C. A., "A Variational Framework for Solution Method Developments in Structural Mechanics," *Journal of Applied Mechanics*, Vol. 65, No. 1, 1998, pp. 242–249.  
<sup>17</sup>Park, K. C., Gumaste, U., and Felippa, C. A., "A Localized Version of the Method of Lagrange Multipliers and Its Applications," *Computational Mechanics: An International Journal*, Vol. 24, No. 6, 2000, pp. 476–490.  
<sup>18</sup>Park, K. C., and Felippa, C. A., "A Variational Principle for the Formulation of Partitioned Structural Systems," *International Journal of Numerical Methods in Engineering*, Vol. 47, 2000, pp. 395–418.  
<sup>19</sup>Gumaste, U., Park, K. C., and Alvin, K. F., "A Family of Implicit Partitioned Time Integration Algorithms for Parallel Analysis of Heterogeneous Structural Systems," *Computational Mechanics: an International Journal*, Vol. 24, No. 6, 2000, pp. 463–475.  
<sup>20</sup>Felippa, C. A., and Park, K. C., "The Construction of Free-Free Flexibility Matrices for Multilevel Structural Analysis," *Computer Methods in Applied Mechanics and Engineering* (to be published).  
<sup>21</sup>Bennighof, J. K., Matthew, F. K., and Muller, M. B., "Extending the Frequency Response Capabilities of Automated Multilevel Substructuring," *AIAA Paper 2000-1574*, 2000. **Q18**  
Bennighof, J. K., and Lehoucq, R. B., "An Automated Multilevel Substructuring Computation in Linear Elastodynamics," preprint Sandia National Lab., 2000; also AMLS (submitted for publication). **Q19**  
Felippa, C. A., and Park, K. C., "The Construction of Free-Free Flexibility Matrices for Multilevel Structural Analysis," *Computer Methods in Applied Mechanics and Engineering*, Vol. 191, No. 19, 20, 2002, pp. 2111–2140. **Q20**

A. Berman  
Associate Editor

## Queries

- Q1.** Give postal/ZIP code.
- Q2.** AIAA style is to set vectors in boldfaced type. Please indicate vectors.
- Q3.** References must be listed in the order they are called out in the text. Please check renumbering.
- Q4.** If single quotes are not in the original quotation, delete; also, delete one period if quote came from single sentence (3 ellipses).
- Q5.** Verify eq. no.
- Q6.** Verify eq. no.
- Q7.** Table set up per AIAA style.
- Q8.** Verify symbol.
- Q9.** Table set up per AIAA style.
- Q10.** The final section should be named "Summary" or "Conclusions." OK as set?
- Q11.** References should not be cited for the first time in the Conclusions/Summary section. Please cite earlier or delete.
- Q12.** Give a title for the Appendix.
- Q13.** If this was subsequently published in an archival source, give full publication information./Give month.
- Q14.** Spell out journal name in full.
- Q15.** Verify pub. location./Give year.
- Q16.** Give month.
- Q17.** Spell out journal name in full.
- Q18.** If this was subsequently published in an archival source, give full publication information./Give month.
- Q19.** Provide location Sandia./Give report number./Give month./Spell out acronym./Any update? Give full details if so./Please cite or delete and renumber references here and in text accordingly.
- Q20.** Please cite or delete and renumber references here and in text accordingly.
- Q21.** If color is to be used for figures, please complete color funding acknowledgment at the end of the proof./Which figure are to be in color?